Stable isotopes in cave ice suggest summer temperatures in East-Central Europe are linked to AMO variability

Carmen-Andreea Bădăluță[1,2,3], Aurel Perșoiu[1,4], Monica Ionita[5], Natalia Piotrowska[6]

[1]Stable Isotope Laboratory, Ștefan cel Mare University, Suceava, 720229, Romania
[2]Department of Geography, Ștefan cel Mare University, Suceava, 720229, Romania
[3]Institute for Geological and Geochemical Research, Research Centre for Astronomy and Earth Sciences MTA, Budapest, 1112, Hungary
[4]Emil Racoviță Institute of Speleology, Romanian Academy, Cluj Napoca, 400006, Romania
[5]Alfred Wegener Institute, Helmholtz Center for Polar and Marine Research, Bremerhaven, 27515, Germany
[6]Institute of Physics, Silesian University of Technology, Gliwice, 44-100, Poland

Correspondence to: Carmen-A. Bădăluță (carmen.badaluta@usm.ro), Aurel Perșoiu (aurel.persoiu@gmail.com)

Abstract. The climate of East-Central Europe (ECE) is the result of the combination of influences originating in the wider North Atlantic realm, the Mediterranean Sea and Western Asia/Siberia. Previous studies have shown that the complex interplay between the large-scale atmospheric patterns across the region result in strongly dissimilar summer and winter conditions on time scales ranging from decades to millennia. To put these into a wider context, long-term climate reconstructions are required, but, largely due to historical reasons, these are lacking in ECE. We address these issues by presenting a high resolution, radiocarbon dated record of summer temperature variations during the last millennium in ECE, based on stable isotope analysis of a 4.84 m long ice core extracted from Focul Viu Ice Cave (Western Carpathians, Romania). Comparisons with both instrumental and proxy-based data indicate that the stable isotope composition of cave ice records changes in summer air temperature and has a similar temporal evolution as that of the Atlantic Multidecadal Oscillation on decadal to multi-decadal times scales, suggesting that changes in the North Atlantic are transferred, likely *via* atmospheric processes towards the wider Northern Hemisphere. On centennial time scales, the data shows little summer temperature differences between the Medieval Warm Period (MWP) and the Little Ice Age (LIA) in Eastern Europe. These findings are contrary to those that show a marked contrast between the two periods in terms of both winter and annual air temperatures, suggesting that the cooling associated with the LIA was likely the result of mainly winter time climatic changes.

1 Introduction

Rapid global warming (IPCC, 2018) and the ensuing suite of climatic changes that it triggers (Coumou and Rahmstorf, 2012) demands a clear understanding of the background mechanisms in order to be able to disentangle natural and anthropogenic processes (Haustein et al., 2017; IPCC, 2018). Especially important are high-resolution reconstructions of the past variability of different climatic variables – seasonal air temperatures, precipitation amounts, moisture sources – that allow for direct comparisons with the dynamics of natural forcing and further deciphering the mechanisms of past and present climate dynamics. The last 1000 years are particularly significant, as the European climate changed from, generally, warm to cold (the Medieval Warm Period-Little Ice Age transition, Jones et al., 2009) and back to warm (the present-day warming, Neukom et al., 2019). These transitions allow for testing the links between forcing and climatic response. While several global (Jones and Mann, 2004; Mann et al, 2009) and hemispheric (Moberg et al, 2005; Neukom et al., 2019; PAGES 2k Consortium, 2019; Ljungqvist et al., 2019) climatic reconstructions have been published, these made no seasonal differentiation – a task that became recently increasingly necessary to constrain seasonally distinctive climatic changes (e.g., Ljungqvist et al., 2019), as these are responding to different forcing mechanisms (e.g., Perșoiu et al., 2019). On multidecadal time scales, summer climate over Europe is influenced, mainly, by the Atlantic Multidecadal Oscillation or AMO

(Schlesinger et al., 1994; Kaplan et al., 1998; Kerr, 2000; Knudsen et al., 2011, 2014). The AMO is a climate mode of variability associated with periodic anomalies of sea surface temperatures (SSTs) in northern, extratropical latitudes. The positive phase is characterized by positive SST anomalies spanning the whole North Atlantic Ocean and is associated with above normal temperature over the central and eastern part of Europe, while the negative phase is characterized by negative SST anomalies over the North Atlantic Ocean and is associated with below normal temperatures over the central and eastern part of Europe. Over Europe the influence of the AMO is clearest during summer (Sutton and Dong, 2012; Ioniță et al., 2012; 2017; O'Reilly et al., 2017).

In temperate climatic region, one of the most sensitive environmental archives are ice caves (Homlund et al., 2005, Kern and Perșoiu, 2013), i.e., rock-caves hosting perennial accumulations of ice. In such caves, ice forms either by freezing of water or direct snow deposition in the entrance shafts (e.g., Mavlyudov, 2018). Several studies have shown that these deposits host a wealth of information on past climate variability. Thus, Stoffel et al. (2009), Perșoiu et al. (2017) and Sancho et al. (2018) have shown that proxies in cave ice forming during winter months record changes in temperature and moisture sources, likely influenced by the dynamics of the North Atlantic Oscillation. Other studies have used pollen and plant macrofossils recovered from cave ice to reconstruct past vegetation dynamics (Feurdean et al., 2011; Leunda et al., 2019) while others used the accumulation rate of ice as indicators of past climatic variability (e.g., Kern et al., 2018) or atmospheric processes (Kern et al., 2009). Studies of ice caves in southern Europe have also highlighted the sensitivity of cave glaciers to summer climatic conditions (Colucci et al., 2016; Colucci and Guglielmin, 2019; Perșoiu et al., 2020). Regardless of the deposition style, the ice records the original stable isotope composition of precipitation that further reflects changes in air temperature and thus is an important archive of past temperature and moisture source variability (Perșoiu et al., 2011a, 2011b). The Carpathian Mountains host ice caves (Bella and Zelinka, 2018; Brad et al., 2018) that preserve a large variety of geochemical information on past climate and environmental changes (Fórizs et al., 2004; Kern et al., 2004; Citterio et al., 2005; Perșoiu et al., 2017). Here, we present a reconstruction of summer climate variability and large-scale circulation drivers during the last 1000 years in East Central Europe based on the $\delta^{18}O$ and $\delta^{2}H$ values measured along an ice core drilled in Focul Viu Ice Cave (Western Carpathian Mountains, Romania).

2 Site information

Focul Viu Ice Cave (FV, 107 m long, ~30 m deep) is located in the Central Bihor Mountains, Romania (46°34'N; 22°40'E, 1165 m above sea level, Fig. 1a, Perșoiu and Onac, 2019). The cave has a simple morphology (Fig. 1b, 1c) with a small entrance that opens into the Great Hall (68 × 46 m), which, in turn, is followed by a narrow gallery (Little Hall, 20 × 5 m). The ceiling of the Great Hall opens to the surface (Fig. 1c) allowing precipitation to reach the cave. Below the opening, and covering the entire surface of the Great Hall, a layered ice block has developed, with an estimated thickness of 20 m and minimum volume of 30,000 m^3 (Orghidan et al., 1984; Brad et al., 2018). The descendent morphology of the cave and the presence of the two openings determine air circulation (Perșoiu and Onac, 2019), with cold air inflow through the lower entrance and warm air outflow through the upper one in winter, and slow convective circulation within the cave (with no air mass exchange with the exterior) during summer. As a result of this air circulation, between October and April the dynamics of air temperature inside and outside of the cave follow a similar pattern while between May and September the temperatures are stable at 0 °C (Perșoiu et al., 2007).

A direct consequence of the predominantly negative air temperatures in the cave is the genesis, accumulation and preservation of ice (Fig. 1b, 1c). During summer, infiltrating rainwater accumulates on top of the existing ice block to form a layer of water, approximately 0-20 cm deep. Monitoring of air temperature in the cave has shown that in early autumn (September) air temperature drop below 0 °C outside the cave leading to cold air avalanches reaching the inner parts of the cave (Perșoiu et al., 2007). The inflow of cold air leads to the freezing of the lake water from top to bottom, forming a 1-20

centimeter thick layer of ice (*summer ice*). Although air temperature might briefly raise above 0 °C in autumn, temperatures inside the cave do not rise above 0 °C. Thus the layer of ice formed on top of the lake will prevent subsequent addition of water to the lake, so that it will preserve the original composition of summer precipitation. Infiltration and subsequent freezing of water during warm periods in winter results in additional layers of ice on top of the ice block (*winter ice*). However, at the onset of melting, this winter ice melts (Perșoiu et al., 2011b). The result of these processes is a multiannual, layered, ice block, consisting of annual couplets of clear ice (on top) and a sediment-rich layer beneath. Inflow of warm water in wet summers leads to rapid ablation of the ice at the top of the ice block, partly altering the annual layering. The processes of cave ice formation by water freezing and the registration of environmental signals by various proxies (e.g., stable isotope composition of ice, pollen content) have been described from the nearby Scărișoara Ice Cave (Perșoiu and Pazdur, 2011; Feurdean et al., 2011) and, given the similarities between the two caves, are also pertinent to Focul Viu Ice Cave. The one notable difference is the timing of the onset of freezing: in Scărișoara Ice Cave, the onset of freezing is delayed until late-autumn and early winter (Perșoiu et al., 2017), whereas in Focul Viu Ice Cave it starts in early autumn.

3 Methods

3.1 Drilling and stable isotope analyses

The FV ice core (4.87 m long, 10 cm diameter) was drilled in May 2016 from the Great Hall of FV Ice Cave (Fig. 1d) using a modified PICO electric drill (Koci and Kuivine, 1984) manufactured by Heavy Duties S.R.L, Cluj Napoca, Romania. A rock embedded in the ice at 4.87 m below the surface stopped the drilling effort, but previous work in the cave has shown that the thickness of the ice block exceeds 15 m (Orghidan et al., 1984; Kern et al., 2004; Perșoiu and Onac, 2019). The ice core was cut into 1 cm long pieces (considering also the annual layering) and subsequently each piece was sealed in plastic bags, allowed to melt at room temperature, transferred to 20 mL HDPE scintillation vials and stored at 4 °C prior to analysis.

Precipitation samples were collected monthly between March 2012 and December 2018 at Gheţar (GT, 46°29'28.45" N, 22°49'26.02" E, 1100 m asl, ~13 km SE of the location of FV Cave) using collectors built according to IAEA specification.

Water samples were analyzed for stable isotope composition at the Stable Isotope Laboratory, Ștefan cel Mare University (Suceava, Romania), using a Picarro L2130*i* CRDS analyzer connected to a high precision vaporizing module. All samples were filtered through 0.45 µm nylon membranes before analysis and manually injected into the vaporization module multiple times, until the standard deviation of the last four injections was less than 0.03 for $\delta^{18}O$ and 0.3 for $\delta^{2}H$, respectively. The average of these last four injections was normalized on the SMOW-SLAP scale using two internal standards calibrated against VSMOW2 and SLAP2 standards provided by the IAEA and used in our interpretation. A third standard was used to check the long-term stability of the analyzer. The stable isotope composition of oxygen and hydrogen are reported using standard δ notation, with precision estimated to be better than 0.1 ‰ for $\delta^{18}O$ and 0.5 ‰ for $\delta^{2}H$ respectively, based on repeated measurements of an internal standard.

3.2 Radiocarbon dating and age-depth model construction

The wide opening to the surface in the ceiling of the Great Hall (Fig. 1c) allows for a large volume of organic matter to fall into the cave and subsequently become trapped in the ice, including large pieces of wood, which tend to cut through layers of ice, sometimes encompassing decades of ice accumulation. Furthermore, ice melting and water freezing processes usually result in inclined ice surfaces and slow tipping of any heavy materials sitting on top of the ice (see the position of tree trunks in Fig. 1). As a consequence, wood with an age older than that of the newly forming ice can be incorporated in the ice block, resulting in sample ages much older than the ice layers ("old wood effect"). However, the challenge to identify such organic material contrasts with the desire for precise chronologies, which rely on high number of data points. Thus, all possible organic samples were recovered and dated, and unreliable ages identified at the stage of age-depth modeling were removed.

Out of 14 samples recovered from the ice core and potentially suitable for radiocarbon dating, two were not datable due to their extremely small carbon yield. AMS radiocarbon analyses were performed at the Institute of Physics, Silesian University of Technology, Poland (Piotrowska, 2013). All samples were precleaned with standard acid-alkali-acid treatment, dried and subjected to graphite preparation using an AGE-3 system (IonPlus, CH) equipped with an Elementar VarioMicroCube elemental analyzer and automated graphitization unit (Wacker et al., 2010; Nemec et al., 2010). The ^{14}C concentrations in graphite produced from unknown samples, Oxalic Acid II standards and coal blanks of comparable carbon masses were measured by the DirectAMS laboratory, Bothell, USA (Zoppi et al., 2007). The results are reported in Table 1. The radiocarbon dates were calibrated using OxCal v4.3 (Bronk Ramsey, 2009) and the IntCal13 calibration curve (Reimer et al., 2013). The NH1 curve (Hua et al., 2013) was used for one post-bomb date.

Because organic material can fall into the cave decades to centuries before being trapped in the ice (see Fig. 1b), we have carefully screened the radiocarbon results prior to age-depth modeling with the aim of selecting the most reliable dates forming a chronological sequence. In total, four dates were selected for age-depth modeling. For the top of the ice core a uniform age distribution from 1991 to 2016 AD was assigned, allowing for the possibility of surface ice melting. The model was constructed using the OxCal *P_Sequence* algorithm (Bronk Ramsey, 2008) with variable prior *k* parameter (*k*=1, U(-2,2); Bronk Ramsey and Lee, 2013) and extrapolated to a depth of 4.86 m. The agreement index of the model was 85 %, confirming a good statistical performance when the threshold of 60 % is surpassed. The sections between the dated depths were assumed to have a constant deposition rate. The complete age-depth model is shown in Fig. 2. For further analysis the mean age derived from the model was used and is also reported in Table 1. The constructed age-depth model was compared with the only reliable one existing for Focul Viu, published by Maggi et al. (2008), which is plotted in green in Fig. 2 and prove a broad agreement of both chronologies. All our rejected ages are older than those of Maggi et al. (2008), and we suspect that these were based on dating old wood that was already in the cave for decades before being incorporated in the ice (see the "old wood effect" discussion above and Fig. 1c). Further, the same authors identified several potential markers of volcanic eruptions and their ages agree within ±40 years with those of our model. Another evaluation was obtained by comparison of our stable isotope record with the one of Kern et al. (2004) and Forizs et al. (2004), and although the latter lack a precise chronology, a simple visual correlation between the records indicates a satisfactory match between the two records. In order to avoid any circular reasoning, we decided against numerical use of other records, e.g. the regional temperature record, to further anchor our chronology.

3.3 Climate data

The sea surface temperature (SST) is extracted from the Extended Reconstructed Sea Surface Temperature data (ERSSTv5) of Huang et al. (2018). This dataset covers the period 1854 – present and has a spatial resolution of 2° x 2°. The AMO index used in this study has been obtained from https://climexp.knmi.nl/data/iamo_ersst_ts.dat and is based also on the ERSSTv5 data set. Station-based meteorological data was provided by the Romanian National Meteorological Administration for three stations (Baia Mare, Sibiu and Timișoara) that have some of the longest instrumental records in Romania and are bracketing the location of the study site. To remove the short-term variability and retain only the multidecadal signal in our data, prior to the correlation analysis, both the temperature time series and the SST data were smoothed with a 21-year running mean filter.

4 Results and discussions

4.1 Ice accumulation in Focul Viu Ice Cave

The results of the radiocarbon analyses performed on organic matter recovered from the ice are shown in Table 1 with the age-depth model shown in Fig. 2. The maximum age of the ice is 1000±20 cal BP at 4.45 m below surface, based on direct dating of organic remains (Table 1) and extrapolated to 1100 cal BP at 4.86 m below surface

High accumulation rates were recorded between AD 850 and 950 (0.39-0.41 cm/year) and between AD 1220 and 1970 (0.36-0.44 cm/year). Between AD 950 and 1220, the net accumulation rate dropped to between 0.29 and 0.34 cm/year. The highest net accumulation rates recorded after AD 1970 (0.56 cm/year) contradict recent findings from other ice caves in the Carpathian Mountains (Kern and Perșoiu, 2013), which all register record melting. However, this value might be an artifact of the depth-age modeling (see above) as well as of the very short time span considered, thus being unreliable for further interpretation. The low accumulation rates spanning the MWP are similar to those recorded in Scărișoara Ice Cave (Perșoiu et al., 2017, Bădăluță, 2019), Hundsalm Ice Cave in Austria (Spötl et al., 2014) and ice caves in Velebit Mountains, Croatia (Kern et al., 2018), potentially suggesting a regional signal of climatic conditions unfavorable for ice accumulation. Ice can melt as a result of either warm summers with enhanced conductive heat transfer to the cave or wet summers, with rapid ablation resulting from water flowing across the top of the ice block. Subsequently, ice growth is influenced by the amount of water present at the onset of freezing, the timing of this onset and its duration. The low accumulation rates during the MWP were likely the result of enhanced melting during warm (see section 4.2 below) and wet (Feurdean et al., 2015) conditions. After AD 1450, the climate in the region was dominated by dry summers with frequent storms and cold winters (Perșoiu, 2017). These conditions lead to reduced summer melting and enhanced winter growth, thus conditions favorable for net ice accumulation.

4.2 Stable isotopes in Focul Viu cave ice - proxy for summer air temperatures and AMO variability

The variability of $\delta^{18}O$ and $\delta^{2}H$ in precipitation at Gheţar (~13 km south of the cave's location and at the same altitude), assessed for the 2012-2017 period, follows that of temperature (Fig. 3a), with the maximum values (-3.6 ‰ and -26 ‰, for $\delta^{18}O$ and $\delta^{2}H$, respectively) in July/August and minimum (-19.8 ‰ and -140 ‰, for $\delta^{18}O$ and $\delta^{2}H$, respectively) in January. Similar result were found by Bojar et al. (2009) and Ersek et al. (2018) for the same region, suggesting that the $^{18}O/^{16}O$ and $^{2}H/^{1}H$ ratios in precipitation register temperature changes on a regional scale. The Local Meteoric Water Line, defined by the equation $\delta^{18}O = 7.4*\delta^{2}H + 6.1$ (Fig. 3b), has a slope and intercept very similar to those found by Ersek et al (2018). Precipitation in the region is mainly delivered by weather systems carrying moisture form the Atlantic Ocean, with the Mediterranean Sea contributing moisture during autumn and winter (Nagavciuc et al, 2019b). The deuterium excess in precipitation (*d-excess* or d), defined as $d = \delta^{2}H - 8*\delta^{18}O$ (Dansgaard, 1964) allows for a clear separation of the air masses: Atlantic ocean (d-excess close to the global average of 10 (Craig, 1961)) and the Mediterranean Sea (d-excess between 12 and 17, resulting from the high evaporative conditions in the Eastern Mediterranean Sea). Similarly high values of *d-excess* have been measured by Drăguşin et al. (2017) in precipitation in southwest Romania and Bădăluță et al. (2019) in precipitation in northeast Romania and linked to air masses originating in the strongly evaporated Mediterranean and Black seas, respectively.

Observations on the dynamics of cave ice during the past 18 years have shown that it starts to grow in early autumn by the freezing of water accumulated during summer. As the ceiling of the cave is opened to the exterior, precipitation directly reaches the site of ice formation, so that the stable isotope composition of precipitation is not modified in the epikarst above the cave thus preserving the original $\delta^{18}O$ and $\delta^{2}H$ values of summer (June-July-August, JJA) precipitation. However, while freezing processes in caves could alter the original $\delta^{18}O$ (and $\delta^{2}H$) values in cave ice, several studies have shown (e.g., in the nearby Scărișoara Ice Cave (Perșoiu et al. (2011b)) that the original climatic signal embedded in the stable isotope composition of cave ice is preserved and can be used as a proxy for external climate variability.

Overall, our observations of cave ice genesis and dynamics and stable isotope monitoring data clearly indicate that summer air temperatures are registered and preserved in the ice block in FV Cave. In order to test the long-term preservation of these connections, we have analyzed the links between the FV $\delta^{18}O_{ice}$ record and instrumental data from three nearby meteorological stations over the AD 1851 – AD 2016 period. On multidecadal time scales, summer air temperature changes in the region are controlled mainly by the dynamics of the Atlantic Multidecadal Oscillation (Ionita et al., 2012). Figure 4 shows the JJA air temperature at Baia Mare (BM), Sibiu (SB) and Timișoara (TM) stations, the AMO index and FV $\delta^{18}O_{ice}$. The instrumental temperature data indicates large multidecadal variability, with a cold period between AD 1890 and 1920, followed by a warm period between AD 1921 and 1960, a slightly colder period between AD 1960 and 1980, and enhanced warming after AD 1980, all following the AMO variability. The $\delta^{18}O_{ice}$ values show a similar temporal evolution, the slight offsets between the observational data and $\delta^{18}O$ being likely due to the dating uncertainty (20 – 35 years). Further, we have computed the correlation map between the summer mean air temperature at SB station (with the longest instrumental record) and the summer SST as indicator of AMO variability (Sutton and Dong, 2012). Figure 5 clearly shows that positive (negative) temperature anomalies over the analyzed region are associated with positive (negative) SST anomalies over the North Atlantic Ocean, resembling the SST anomalies associated with the positive (negative) phase of AMO (Mesta-Nuñez and Enfield 1999, Latif et al. 2004; Knight et al. 2005). The strongest correlations (Fig. 5) are found between SSTs in the North Atlantic and the Eastern Mediterranean Sea, both being the main sources of moisture feeding local precipitation (Bădăluță et al., 2019). These results are also in agreement with the results of Della-Marta et al. (2007), showing that summer positive temperature anomalies and heatwaves over Europe are triggered, at least partially, by the phase of AMO. A recent study of $\delta^{18}O$ variability in oak tree rings in NW Romania (~50 km NW from our site) also indicates the influence of the AMO on summer temperatures and drought conditions (Nagavciuc et al., 2019a). Thus, we suggest that, during summer, strongly meandering Rossby waves (Ionita et al., 2015, 2017) result in blocking conditions over Central Europe that lead to the persistence of high-pressure systems and occurrence of regional heat waves. These, in turn, favor regional recycling of moisture resulting in positive $\delta^{18}O$ anomalies in precipitation that are further recorded by cave ice (this study) and tree rings (Popa and Kern, 2009; Nagavciuc et al., 2019a). Hmbqd`rdc bnmsqhat shnm ne qdbxbkdc l nhrst qd sn oqdbhohs`shnm g`r addm qdonqsdc hmBdmsq`kDt qnod+et qsgdqrt oonqshmf`nt qhmedqdmbd'Fńl dy-Gdqḿndez et al., 2013; Kern et al., 2020).

Combining all data above, it results that on time scales ranging from years to decades, prolonged periods of positive temperature anomalies throughout the summer months, linked to prolonged warm SSTs in the North Atlantic Ocean (and thus a positive AMO index), could be preserved by the $\delta^{18}O_{ice}$ in FV Ice Cave.

The FV $\delta^{18}O_{ice}$ and $\delta^{2}H_{ice}$ records span the AD 850 – AD 2016 period. Decadal to multi-decadal scale oscillations occur over the entire record, but no discernable long-term trend was identified. Several periods of excursions towards low $\delta^{18}O$ values (defined as $\delta^{18}O_{ice}$ below the long term average, suggesting low summer temperatures) dot the past 1100 years at AD 875-930, AD 1050-1080, AD 1260-1330, AD 1430-1480, AD 1520-1550, AD 1710-1750, AD 1820-1870, AD 1880-1930. Significant maxima in the FV $\delta^{18}O_{ice}$ record occurred between AD 850-870, AD 1000-1050, AD 1080-1260, AD 1350-1390, AD 1480-1520, AD 1625-1710, AD 1950-1970 (Fig. 6). Both $\delta^{18}O_{ice}$ and $\delta^{2}H_{ice}$ records display a remarkable similarity throughout the entire period and in our discussion we have relied on the $\delta^{18}O$ record, only. We have compared the FV $\delta^{18}O_{ice}$ with tree ring width-based reconstruction of summer (JJA) temperature anomalies from the Eastern Carpathian Mountains (Popa and Kern, 2009). The highest similarities between the FV ice core and summer temperature records were found for the cold periods between AD 1260-1330, AD 1430-1480, AD 1520-1550 and AD 1820-1870 and the warm periods during AD 1080 – 1260, AD 1625-1710, AD 1950-1970 (Fig. 6). Given the very different nature of the two archives (trees versus cave ice), of the proxies (tree rings and $\delta^{18}O$) and of the chronologies (annual tree ring counting vs. ^{14}C dating with a ± 30 years error), the two records agree remarkably well, further supporting the hypothesis that $\delta^{18}O$ and $\delta^{2}H$ values in FV ice core is

registering both summer air temperature variability during the past ca. 1000 years in East-Central Europe, as well as, on a broader spatial scale, the variability of the AMO.

Similar to the AD 1850-2016 interval described above, the stable isotope record closely mirrors the AMO variability over the entire studied interval (Fig. 7). The relationship between the FV $\delta^{18}O_{ice}$ and AMO records is strongest between AD 1125 and AD 1525 and AD 1750 and AD 2016, with decadal-scale variability in the two records being synchronous. Peak-to-peak matching of the FV $\delta^{18}O_{ice}$ and AMO records shows that during the past 1000 years the two records correlated well within the dating uncertainty (±30 years). However, between ~AD 1600 and 1750 (Fig. 7) peak-to-peak matching indicates a difference between the two records up ~ 50 years, likely the result of high (> 50 years) uncertainty in the ice core chronology between AD 1525 and AD 1750 (Fig. 7a). The overall correlations between 1) FV $\delta^{18}O_{ice}$ and instrumental summer temperature reconstruction over the past 150 years, 2) the instrumental (this study) and proxy-based (Nagavciuc et al., 2019a) correlations between summer air temperatures and AMO variability and 3) the correlations between the FV $\delta^{18}O_{ice}$ and AMO records over the past 1000 years suggest that changes in the North Atlantic are transferred, likely *via* atmospheric processes, towards the wider Northern Hemisphere, resulting in hemispheric-wide climatic responses to perturbations in the North Atlantic.

The FV $\delta^{18}O_{ice}$ record is in agreement with other summer temperature reconstructions (e.g., Buntgen et al., 2011) at regional and hemispheric scale (Fig. 6). Further, regional summer temperature (e.g., Popa and Kern, 2009) and summer temperature-sensitive drought (Seim et al., 2012) reconstructions show warm peaks around AD 1320, 1420, 1560, 1780 and cooling around AD 1260, 1450 and 1820, similar with reconstructions and models at global level (Neukom et al., 2019) and the FV temperature reconstruction (this study). Contrary to the summer season temperature reconstructions, a late-autumn through early winter season temperature reconstructions from the nearby Scărișoara Ice Cave (Perșoiu et al., 2017) shows that the MWP was rather warm and also wet (Feurdean et al., 2011), while the LIA was cold, and likely drier and with erratically distributed precipitation. Together, these data suggest a complex picture of climate variability in the wider Carpathian region, with much of the yearly temperature variability during the past 1000 years being attributed to the influence of winter conditions, summer temperatures being rather constant.

5 Conclusions

The analysis of the oxygen and hydrogen stable isotope ratios along a ~5 m long ice core extracted from Focul Viu Ice Cave (northwest Romania) provided an unprecedented view on the dynamics of summer air temperature and atmospheric circulation changes during the past 1000 years in East-Central Europe. Comparison of ice core $\delta^{18}O$ (and $\delta^{2}H$) with instrumental data over the past 150 years indicates that the stable isotope composition of cave ice records summer air temperatures on multidecadal time-scales. Given the apparent relationship between our stable isotope record and both instrumental and proxy-derived records of the Atlantic Multidecadal Oscillation (AMO) we further suggest that $\delta^{18}O_{ice}$ in Focul Viu Ice Cave can be used to infer past AMO variability. We subsequently hypothesize that changes in summer climatic conditions over the Northern Atlantic are transferred through atmospheric processes across the Northern Hemisphere, influencing summer temperatures across Europe. However, we emphasize that given the ±30 years uncertainty in the chronology, detailed studies using better constrained age models (e.g., tree ring-based proxies) are required to test this hypothesis.

The data shows little centennial-scale summer temperature variability since the onset of the Medieval Warm Period and through the Little Ice Age. Nevertheless, well-expressed minima and maxima occurred synchronously with data from other records in the region and through Europe, suggesting that the stable isotope composition from cave ice records a regional climatic signal. Contrary, winter air temperature records from the region indicate colder conditions during the LAI compared

to the MWW, pointing towards a seasonally distinct climatic signal during these two periods. This suggests that forcing factors acting seasonally had a strong imprint on temperature variability, overriding long-term, global forcing.

Our results offer a potential hypothesis to be further tested by extending this and similar records back in time and also incorporate other proxy-base reconstructions to investigate the spatial extent of the influence of North Atlantic climate further east.

Author contributions. CAB and AP designed the project, AP and CAB collected the ice core and CAB performed the stable isotope analyses. NP performed the radiocarbon analyses and constructed the depth-age model. MI analyzed the climate and large-scale circulation data. CAB and AP wrote the text, with input from MI and NP.

Competing interests. The authors declare that they have no conflict of interest.

Data availability. The Focul Viu $\delta^{18}O$ and $\delta^{2}H$, as well as the ^{14}C data and the modeled ages will be made available upon publication, both on the CP webpage and on the NOAA/World Data Service for Paleoclimatology webpage. The meteorological data plotted in figure 4 was provided by the Romanian National Meteorological Administration, except for the AMO data (panel a) which was downloaded from https://climexp.knmi.nl/data/iamo_ersst_ts.dat. The paleoclimate data used to plot fig. 7, panels a, b, c, d and e was downloaded from the NOAA/World Data Service for Paleoclimatology webpage.

Acknowledgments. The research leading to these results has received funding from EEA Financial Mechanism 2009- 2014 under the project contract no CLIMFOR18SEE. AP was partial financially supported by UEFISCDI Romania through grants no. PN-III-P1-1.1-TE-2016-2210, PNII-RU-TE-2014-4-1993 and SEE 126/2018 KARSTHIVES. MI was partially supported by the AWI Strategy Fund Project PalEX and by the Polar Regions and Coasts in the Changing Earth System (PACES) program of the AWI. We thank the Administration of the Apuseni National Park for granting permission to drill in Focul Viu Ice Cave, Nicodim Pașca for collecting precipitation samples, dr. Christian Ciubotărescu for help during the ice core drilling effort and Vlad Murariu (Heavy Duties Romania) for developing and constructing the drilling equipment. We thank the editor and three anonymous reviewers for comments that helped us improve the original manuscript and dr. Simon Hutchinson (University of Salford, UK) and Sara Asha Burgess for further suggestions and corrections.

Financial support. The article processing charges for this open-access publication were covered by the project EXCALIBUR of the Ștefan cel Mare University of Suceava, Romania.

References

Bădăluță C.–A: Reconstruction of air temperature during the last 1000 years based on the stable isotope analysis of ice deposits in caves from the Apuseni Mountains, Romania, PhD thesis, Stefan cel Mare University of Suceava, 2019.

Bădăluță, C.–A., Persoiu, A., Ionita, M., Nagavciuc, V., and Bistricean, P. I.: Stable H and O isotope-based investigation of moisture sources and their role in river and groundwater recharge in the NE Carpathian Mountains, East-Central Europe, Isot. Environ. Healt. S., 55 (2), 161–178, https://doi.org/10.1080/10256016.2019.1588895, 2019.

Brad, T., Bădăluță C.-A., and Persoiu, A.: Ice caves in Romania, in: Ice caves, edited by: Perșoiu, A. and Lauritzen, S.-E., Elsevier, Amsterdam, Netherlands, 511–528, https://doi.org/10.1016/B978-0-12-811739-2.00025-5, 2018.

Bojar, A, Ottner, F, Bojar, H. P., Grigorescu, D., and Persoiu, A.: Stable isotope and mineralogical investigations on clays from the Late Cretaceous sequences, Hațeg Basin, Romania, Appl. Clay Sci., 45, 155–163, https://doi.org/10.1016/j.clay.2009.04.005, 2009.

Bronk Ramsey, C. and Lee, S.: Recent and Planned Developments of the Program OxCal, Radiocarbon, 55, 720–730, https://doi.org/10.1017/S0033822200057878, 2013.

Bronk Ramsey, C.: Bayesian analysis of radiocarbon dates, Radiocarbon, 51, 337–360, 2009.

Bronk Ramsey, C.: Deposition models for chronological records, Quaternary Sci. Rev., 27, 42–60, https://doi.org/10.1016/j.quascirev.2007.01.019, 2008.

Büntgen, U., Tegel, W., Nicolussi, K., McCormick, M., Frank, D., Trouet, V., Kaplan, J. O., Herzig, F., Heussner, K-U., Wanner, H., Luterbacher, J., and Esper, J.: 2500 Years of European Climate Variability and Human Susceptibility, Science, 331, 578–582, https://doi.org/10.1126/science.1197175, 2011.

Citterio, M., Turri, S., Perșoiu, A., Bini, A., and Maggi, V.: Radiocarbon ages from two ice caves in the Italian Alps and the Romanian Carpathians and their significance, In: Glacier Caves and Glacial Karst in High Mountains and Polar Regions, edited by: Mavlyudov, B. R., Institute of geography of the Russian Academy of Sciences, Moscow, Russia, 87–92, 2005.

Colucci, R. R., and Guglielmin, M.: Climate change and rapid ice melt: Suggestions from abrupt permafrost degradation and ice melting in an alpine ice cave, Progress in Physical Geography: Earth and Environment, 43, 561-573, 10.1177/0309133319846056, 2019.

Colucci, R. R., Fontana, D., Forte, E., Potleca, M., and Guglielmin, M.: Response of ice caves to weather extremes in the southeastern Alps, Europe, Geomorphology, 261, 1-11, http://dx.doi.org/10.1016/j.geomorph.2016.02.017, 2016.

Coumou, D., and Rahmstorf, S.: A decade of weather extremes, Nat. Clim. Change, 2, 491–496, https://doi.org/10.1038/nclimate1452, 2012.

Craig, H.: Isotopic variations in meteoric waters, Science, 133, 1702–1703, https://doi.org/10.1126/science.133.3465.1702, 1961.

D'Arrigo, R., Wilson, R., and Jacoby G.: On the long-term context for late twentieth century warming, J. Geophys. Res., 111, D03103, https://doi.org/10.1029/2005JD006352, 2006.

Dansgaard, W.: Stable isotope in precipitation, Tellus, 16, 436–438, https://doi.org/10.1111/j.2153-3490.1964.tb00181.x, 1964.

Della-Marta, P. M., Luterbacher, J., von Weissenfluh, H., Xoplaki, E., Brunet, M., and Wanner, H.: Summer heat waves over western Europe 1880–2003, their relationship to large scale forcings and predictability, Clim. Dynam., 29, 251–275, https://doi.org/10.1007/s00382-007-0233-1, 2007.

Dragusin, V., Balan, S., Blamart, D., Forray, F. L., Marin, C., Mirea, I., Nagavciuc, V., Persoiu, A., Tirla, L., Tudorache, A., and Vlaicu, M.: Transfer of environmental signals from surface to the underground at Ascunsă Cave, Romania, Hydrol. Earth Syst. Sci., 21, 5357–5373, https://doi.org/10.5194/hess-21-5357-2017, 2017.

Feurdean, A., Persoiu, A., Pazdur, A., and Onac, B. P.: Evaluating the palaeoecological potential of pollen recovered from ice in caves: a case study from Scarisoara Ice Cave, Romania, Rev. Palaeobot. Palyno., 165, 1–10, https://doi.org/10.1016/j.revpalbo.2011.01.007, 2011.

Feurdean, A., Galka, M, Kuske, E., Tanțău, I., Lamentowicz, M., Florescu, G., Liakka, J., Hutchinson, S. M., Mulch, A., and Hickler, T.: Last Millennium hydro-climate variability in Central Eastern Europe (Northern Carpathians, Romania), Holocene, 25, 1179–1192, https://doi.org/10.1177/0959683615580197, 2015.

Fórizs, I., Kern, Z., Szántó, Zs., Nagy, B., Palcsu, L., Molnár, M.: Environmental isotopes study on perennial ice in the Focul Viu Ice Cave, Bihor Mountains, Romania. Theor. App. Karst.17, 61–69, 2004.

Gómez-Hernández, M.; Drumond, A.; Gimeno, L.; Garcia-Herrera, R. Variability of moisture sources in the Mediterranean region during the period 1980–2000. *Water Resour. Res.*, *49*, 6781–6794, 2013.

Haustein, K., Allen, M. R., Forster, P. M., Otto, F. E. L., Mitchell, D. M., Matthews, H. D., and Frame, D. J.: A real-time Global Warming Index, Sci. Rep., 7: 15417, https://doi.org/10.1038/s41598-017-14828-5, 2017.

Holmlund, P., Onac, B. P., Hansson, M., Holmgren, K., Morth, M., Nyman, M., and Persoiu, A.: Assessing the palaeoclimate potential of cave glaciers: the example of the Scărișoara Ice Cave (Romania), Geogr. Ann. A, 87A, 193–201, https://doi.org/10.1111/j.0435-3676.2005.00252.x, 2005.

Hua, Q., Barbetti, M., and Rakowski, A. Z.: Atmospheric Radiocarbon for the Period 1950–2010, Radiocarbon, 55, 2059–2072, https://doi.org/10.2458/azu_js_rc.v55i2.1, 2013.

Huang, B., Angel, W., Boyer, T., Cheng, L., Chepurin, G., Freeman, E., Liu, C., and Zhang, H.-M.: Evaluating SST analyses with independent ocean profile observations, J. Climate, 31, 5015–5030, https://doi.org/10.1175/JCLI-D-17-0824.1, 2018.

IPCC: Global warming of 1.5°C. An IPCC Special Report. Geneva, Switzerland, https://doi.org/10.1017/CBO9781107415324, 2018.

Ionita M**.**, Boroneant, C. and Chelcea, S. : Seasonal modes of dryness and wetness variability over Europe and their connections with large scale atmospheric circulation and global sea surface temperature. *Climate Dynamics*, 45: 2803. https://doi.org/10.1007/s00382-015-2508-2, 2015.

Ionita M., Tallaksen, L.M., Kingston, D. Stagge, J.H., Laaha, G., Van Lanen, H., Scholz, P., Chelcea, S., and Haslinger, K. : The European 2015 drought from a climatological perspective. Hydrology and Earth System Sciences, 21, 1397-1419. doi:10.5194/hess-21-1397-2017, 2017.

Ionita, M., Rimbu, N., Chelcea, S., and Patrut, S.: Multidecadal variability of summer temperature over Romania and its relation with Atlantic Multidecadal Oscillation, Theor. Appl. Climatol., 113, 305–315, https://doi.org/10.1007/s00704-012-0786-8, 2012.

Jones, P. D., Osborn, T. J., and Briffa, K. R.: The evolution of climate over the last millennium, Science, 292(5517), 662-667, https://doi.org/10.1126/science.1059126, 2001.

Jones, P. D., and Mann, M. E.: Climate over the past millennia, Rev. Geophys., 42, RG2002, https://doi.org/10.1029/2003RG000143, 2004.

Jones, P. D., Briffa, K. R., Osborn, T. J., Lough, J. M., van Ommen, T. D., Vinther, B. M., Luterbacher, J., Wahl, E. R., Zwiers, F. W., Mann, M. E., Schmidt, G. A., Ammann, C. M., Buckley, B. M., Cobb, K. M., Esper, J., Goosse, H., Graham, N., Jansen, E., Kiefer, T., Kull, C., Küttel, M., Mosley-Thompson, E., Overpeck, J. T., Riedwyl, N., Schulz, M., Tudhope, A. W., Villalba, R., Wanner, H., Wolff, E., and Xoplaki, E.: High-resolution palaeoclimatology of the

last millennium: A review of current status and future prospects, The Holocene, 19, 3–49, https://doi.org/10.1177/0959683608098952, 2009.

Kaplan, A., Cane, M.A., Cushnir, Y., Clement, A.C., Blumenthal, M.B., and Rajagopala, B., Analyses of global sea surface temperature 1856-1991, Journal of Geophysical Research, 103, 18567 – 18589, 1998.Kern, Z., and Persoiu, A.: Cave ice - the imminent loss of untapped mid-latitude cryospheric palaeoenvironmental archives, Quaternary Sci. Rev., 67, 1-7, https://doi.org/10.1016/j.quascirev.2013.01.008, 2013.

Kern, Z., Fórizs, I., Nagy, B., Kázmér, M., Gál, A., Szánto, Z., Palcsu, L., and Molnár, M.: Late Holocene environmental changes recorded at Gheţarul de la Focul Viu, Bihor Mountains, Romania, Theor. App. Karst., 17, 51–60, 2004.

Kern, Z., Molnár, M., Svingor, É., Persoiu, A., and Nagy, B.: High-resolution, well-preserved tritium record in the ice of Bortig Ice Cave, Bihor Mountains, Romania, The Holocene, 19, 729-736, https://doi.org/10.1177/0959683609105296, 2009.

Kern, Z., Bočić, N., and Sipos, G.: Radiocarbon-Dated Vegetal Remains from the Cave Ice Deposits of Velebit Mountain, Croatia, Radiocarbon, 60, 1391-1402, https://doi.org/10.1017/RDC.2018.108, 2018.

Kern, Z.; Hatvani, I.G.; Czuppon, G.; Fórizs, I.; Erdélyi, D.; Kanduč, T.; Palcsu, L.; Vreča, P. Isotopic 'Altitude' and 'Continental' Effects in Modern Precipitation across the Adriatic–Pannonian Region. *Water* **2020**, *12*, 1797 https://doi.org/10.3390/w12061797.

Kerr, R.A.: A North Atlantic Climate Pacemaker for the Centuries, Science, 288, 1984-1985, DOI: 10.1126/science.288.5473.1984.

Kilbourne, K. H., Alexander, M. A., and Nye, J. A.: A low latitude paleoclimate perspective on Atlantic multidecadal variability, J. Marine Syst., 133, 4–13, https://doi.org/10.1016/j.jmarsys.2013.09.004, 2013.

Knight, J. R., Allan, R. J., Folland, C. K., Vellinga, M., and Mann, M.E.: A signature of persistent natural thermohaline circulation cycles in observed climate, Geophys. Res. Lett., 32, L20708, https://doi.org/10.1029/2005GL024233, 2005.

Knudsen, M., Seidenkrantz, M., Jacobsen, B. et al. Tracking the Atlantic Multidecadal Oscillation through the last 8,000 years. Nat Commun 2, 178, https://doi.org/10.1038/ncomms1186, 2011.

Knudsen, M. F., Jacobsen B. H., Seidenkrantz, M.-S., and Olsen, J.: Evidence for external forcing of the Atlantic Multidecadal Oscillation since termination of the Little Ice Age, Nat. Commun., 5: 3323, https://doi.org/10.1038/ncomms4323, 2014.

Koci, B. R., and Kuivinen, K. C.: The PICO lightweight coring auger, J. Glaciol., 30, 244–245, https://doi.org/10.3189/S0022143000006018, 1984.

Latif, M., Botset, E. R. M., Esch, M., Haak, H., Hagemann, S., Jungclaus, J., Legutke, S., Marsland, S., and Mikolajewicz, U.: Reconstructing, monitoring and predicting multidecadal-scale changes in the North Atlantic thermohaline circulation with sea surface temperature, J. Climate, 17, 1605–1614, https://doi.org/10.1175/1520-0442(2004)017<1605:RMAPMC>2.0.CO;2, 2004.

Leunda, M., González-Sampériz, P., Gil-Romera, G., Bartolomé, M., Belmonte-Ribas, Á., Gómez-García, D., Kaltenrieder, P., Rubiales, J. M., Schwörer, C., Tinner, W., Morales-Molino, C., and Sancho, C.: Ice cave reveals environmental forcing of long-term Pyrenean tree line dynamics, J. Ecol., 107, 814-828, https://doi.org/10.1111/1365-2745.13077, 2019.

Ljungqvist, F. C., Seim, A., Krusic, P. J., González-Rouco, J. F., Werner, J. P., Cook, E. R., Zorita, E., Luterbacher, J., Xoplaki, E., Destouni, G., García-Bustamante, E., Aguilar, C. A. M., Seftigen, K., Wang, J., Gagen, M. H., Esper, J., Solomina, O., Fleitmann, D., and Büntgen, U.: European warm-season temperature and hydroclimate since 850 CE, Environ. Res. Lett., 14, 084015, https://doi.org/10.1088/1748-9326/ab2c7e, 2019.

Maggi, V., Turri, S., Bini, A., and Udisti, R.: 2500 Years of history in Focul Viu Ice Cave, Romania, In: Proceedings of the 3rd International Workshop on Ice Caves, edited by: Kadebskaya, O., Mavlyudov, B., and Patunin, M., Kungur Ice Cave, Russia, 11–15, 2008.

Mann, M. E., Zhang, Z., Rutherford, S., Bradley, R., Hughes, M. K., Shindell, D., Ammann, C., Faluvegi, G., and Ni, F.: Global signatures and dynamical origins of the Little Ice Age and Medieval Climate Anomaly, Science, 326, 1256–1260, https://doi.org/10.1126/science.117730, 2009.

Mavlyudov, B. R.: Ice genesis and types of ice caves, in: Ice caves, edited by: Perşoiu, A. and Lauritzen, S. E., 34-68, https://doi.org/10.1016/B978-0-12-811739-2.00032-2, 2018.

Mesta-Nuñez, A. M., and Enfield, D. B.: Rotated global modes of non-ENSO sea surface temperature variability, J. Climate, 12, 2734–2746, https://doi.org/10.1175/1520-0442(1999)012<2734:RGMONE>2.0.CO;2, 1999.

Moberg, A., Sonechkin, D. M., Holmgren, K., Datsenko, N. M. and Karlén, W.: Highly variable Northern Hemisphere temperatures reconstructed from low- and high-resolution proxy data, Nature, 433, 613-617, https://doi.org/10.1038/nature03265, 2005.

Nagavciuc V., Bădăluță C.-A., Ionita M.: Tracing the Relationship between Precipitation and River Water in the Northern Carpathians Base on the Evaluation of Water Isotope Data, Geosciences, *9*, 198; https://doi.org/10.3390/geosciences9050198, 2019.

Nagavciuc, V., Ionita, M., Persoiu, A., Popa, I., Loader, N. J., and McCarroll, D.: Stable oxygen isotopes in Romanian oak tree rings record summer droughts and associated large-scale circulation patterns over Europe, Clim. Dynam., 52, 6557–6568, https://doi.org/10.1007/s00382-018-4530-7, 2019a.

Nemec, M., Wacker, L., and Gäggeler, H. W.: Optimization of the Graphitization Process at AGE-1, Radiocarbon, 52, 1380–1393, 2010.

Neukom, R., Steiger, N., Gómez-Navarro, J.J., Wang, J. and Werner, J. P.: No evidence for globally coherent warm and cold periods over the preindustrial Common Era, Nature, 571, 550–554, https://doi.org/10.1038/s41586-019-1401-2, 2019.

Orghidan, T., Negrea, Ş., Racoviță, G., and Lascu, C.: Peşteri din România: ghid turistic. Ed. Sport-Turism, Bucureşti, 1984.

O'Reilly, C. H., Woollings, T., and Zanna, L.: The Dynamical Influence of the Atlantic Multidecadal Oscillation on Continental Climate, J. Climate, 30, 7213–7230, https://doi.org/10.1175/JCLI-D-16-0345.1, 2017.

PAGES 2K Consortium: Consistent multidecadal variability in global temperature reconstructions and simulations over the Common Era, Nat. Geosci., 12, 643–649, https://doi.org/10.1038/s41561-019-0400-0, 2019.

Persoiu, A.: Climate evolution during the Late Glacial and the Holocene. In: Landform dynamics and evolution in Romania, edited by: Rădoane, M., and Vespremeanu-Stroe, A., Springer, Berlin, Heidelberg, Germany, 57–66. https://doi.org/10.1007/978-3-319-32589-7_3, 2017.

Persoiu, A., and Pazdur, A: Ice genesis and its long-term dynamics in Scărișoara Ice Cave, Romania, The Cryosphere, 5, 45–53, https://doi.org/0.5194/tc-5-45-2011, 2011.

Persoiu, A., and Onac, B. P.: Ice caves in Romania, In: Cave and Karst Systems of Romania, edited by: Ponta, G. M. L., and Onac, B. P., Springer, Berlin, Heidelberg, Germany, 455–465, https://doi.org/10.1007/978-3-319-90747-5_52, 2019.

Perşoiu A, Feier I, Citterio M, Turri S, Maggi V, 2007, Preliminary data on air temperature in Focul Viu Ice Cave (Bihor Mts., Romania). In (Zelinka, J., ed.) Proceedings of the 2nd International Workshop on Ice Cave, Demänovská dolina, Slovak Republic, 62-64.

Persoiu, A., Onac, B. P., and Perşoiu, I.: The interplay between air temperature and ice dynamics in Scărișoara Ice Cave, Romania. Acta Carsologica, 40, 445–456, https://doi.org/10.3986/ac.v40i3.4, 2011a.

Persoiu, A., Onac, B. P., Wynn, J. G., Bojar, A.-V., and Holmgren, K.: Stable isotope behavior during cave ice formation by water freezing in Scărişoara Ice Cave, Romania, J. Geophys. Res., 116, D02111, https://doi.org/10.1029/2010JD014477, 2011b.

Persoiu, A, Onac, B. P., Wynn, J. G., Blaauw, M., Ionita, M., and Hansson, M.: Holocene winter climate variability in Central and Eastern Europe, Sci. Rep., 7: 1196, https://doi.org/10.1038/s41598-017-01397-w, 2017.

Persoiu, A., Ionita, M., and Weiss H.: Atmospheric blocking induced by the strengthened Siberian High led to drying in the Middle East during the 4.2 ka event –a hypothesis, Clim. Past, 15, 781–793, https://doi.org/10.5194/cp-2018-161, 2019.

Persoiu, A., Buzjak, N., Onaca, A., Pennos, C., Sotiriadis, Y., Ionita, M., Zachariadis, S., Kosutnik, J., Hegyi, A., and Butorac, V.: Accelerated loss of surface and cave ice in SE Europe related to heavy summer rains, The Cryosphere, under review.

Piotrowska, N.: Status report of AMS sample preparation laboratory at GADAM Centre, Gliwice, Poland, Nuclear Instruments and Methods in Physics Research Section B, 294, 176–181, 2013.

Popa, I., and Kern, Z.: Long-Term Summer Temperature Reconstruction Inferred from Tree-ring Records from the Eastern Carpathians, Clim. Dyn., 32, 1107–1117, https://doi.org/10.1007/s00382-008-0439-x, 2009.

Reimer, P. J., Bard, E., Bayliss, A., Beck, J. W., Blackwell, P. G., Bronk Ramsey, C., Grootes, P. M., Guilderson, T. P., Haflidason, H., Hajdas, I., Hatte, C., Heaton, T. J., Hoffmann, D. L., Hogg, A. G., Hughen, K. A., Kaiser, K. F., Kromer, B., Manning, S. W., Niu, M., Reimer, R. W., Richards, D. A., Scott, E. M., Southon, J. R., Staff, R. A., Turney, C. S. M., and van der Plicht J.: IntCal13 and Marine13 Radiocarbon Age Calibration Curves 0-50,000 Years cal BP, Radiocarbon, 55, 1869–1887, https://doi.org/10.2458/azu_js_rc.55.16947, 2013.

Schlesinger, M., and Ramankutty, N.: An oscillation in the global climate system of period 65–70 years. Nature 367, 723–726, , https://doi.org/10.1038/367723a0, 1994.

Sancho, C., Belmonte, Á., Bartolomé, M., Moreno, A., Leunda, M., and López-Martínez, J.: Middle-to-late Holocene palaeoenvironmental reconstruction from the A294 ice-cave record (Central Pyrenees, northern Spain), Earth Planet. Sci. Lett., 484, 135-144, https://doi.org/10.1016/j.epsl.2017.12.027, 2018.

Seim, A., Büntgen, U., Fonti, P., Haska, H., Herzig, F., Tegel, W., Trouet, V., and Treydte, K.: Climate sensitivity of a millennium-long pine chronology from Albania, Clim. Res., 51, 217–228, https://doi.org/10.3354/cr01076, 2012.

Spötl, C., Reimer, P. J., and Luetscher, M.: Long-term mass balance of perennial firn and ice in an Alpine cave (Austria): Constraints from radiocarbon-dated wood fragments, The Holocene, 24, 165-175, doi:10.1177/0959683613515729, 2014.

Stoffel, M., Luetscher, M., Bollschweiler, M., et al.: Evidence of NAO control on subsurface ice accumulation in a 1200 yr. old cave-ice sequence, St. Livres ice cave, Switzerland. Quaternary Research, 72, 16–26, https://doi.org/10.1016/j.yqres.2009.03.002, 2009.

Sutton, R. T., and Dong, B.: Atlantic Ocean influence on a shift in European climate in the 1990s, Nat. Geosci., 5, 788–792, https://doi.org/10.1038/ngeo1595, 2012.

Wacker, L., Nemec, M., and Bourquin, J.: A revolutionary graphitisation system: Fully automated, compact and simple, Nucl. Instrum. Meth. B, 268 (7-8), 931–934, 2010.

Wang, J., Yang, B., Ljungqvist, F. C., Luterbacher, J., Osborn, T.J., Briffa, K. R., and Zorita, E.: Internal and external forcing of multidecadal Atlantic climate variability over the past 1,200 years, Nat. Geosci., 10, 512–517, https://doi.org/10.1038/ngeo2962, 2017.

Zoppi, U., Crye, J., Song, Q., and Arjomand A.: Performance evaluation of the new AMS system at Accium BioSciences, Radiocarbon, 49, 173–182, 2007.

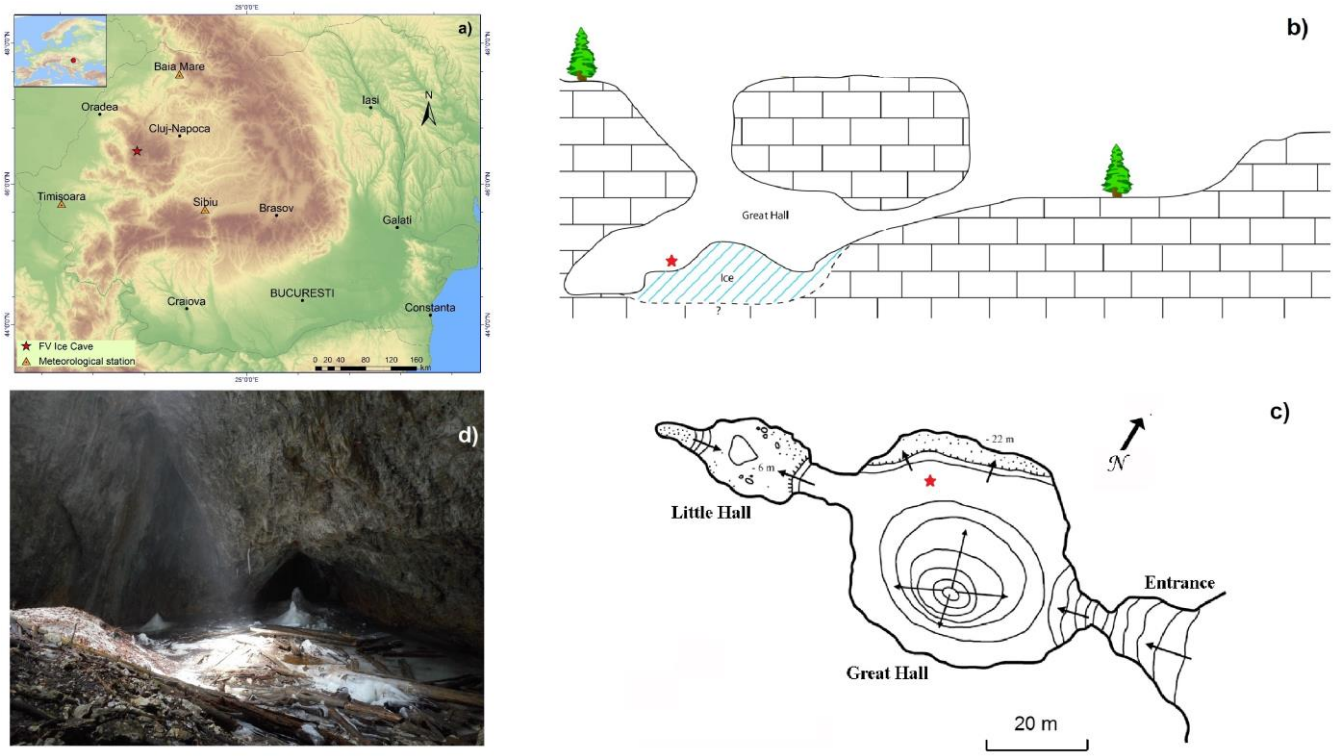

Figure 1. Location of the Focul Viu Ice Cave (red star) in Europe (a),cross section (b) and map (c) of the cave (red star indicates the drilling site) and (d) general view of the Great Hall (person in yellow on the left is standing at the drilling site).

5

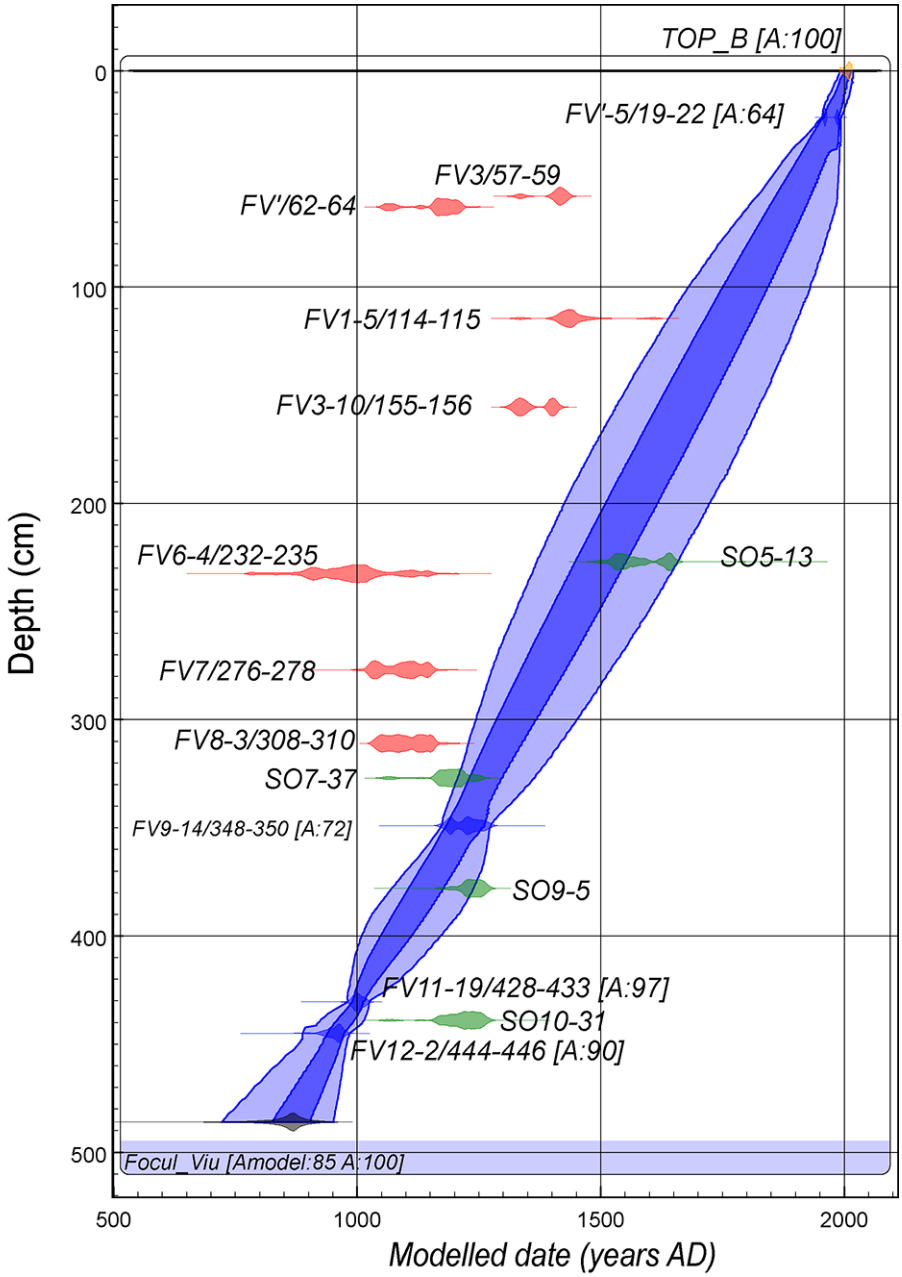

Figure 2. Age-depth model of the Focul Viu ice core. The calibrated age range of samples used in the model is indicated in blue and for those rejected, in red. Samples in green are from the ice core drilled in 2004 (Maggi et al., 2008). Dark and light blue shading indicate the 95 % and 68 % confidence ranges of the model.

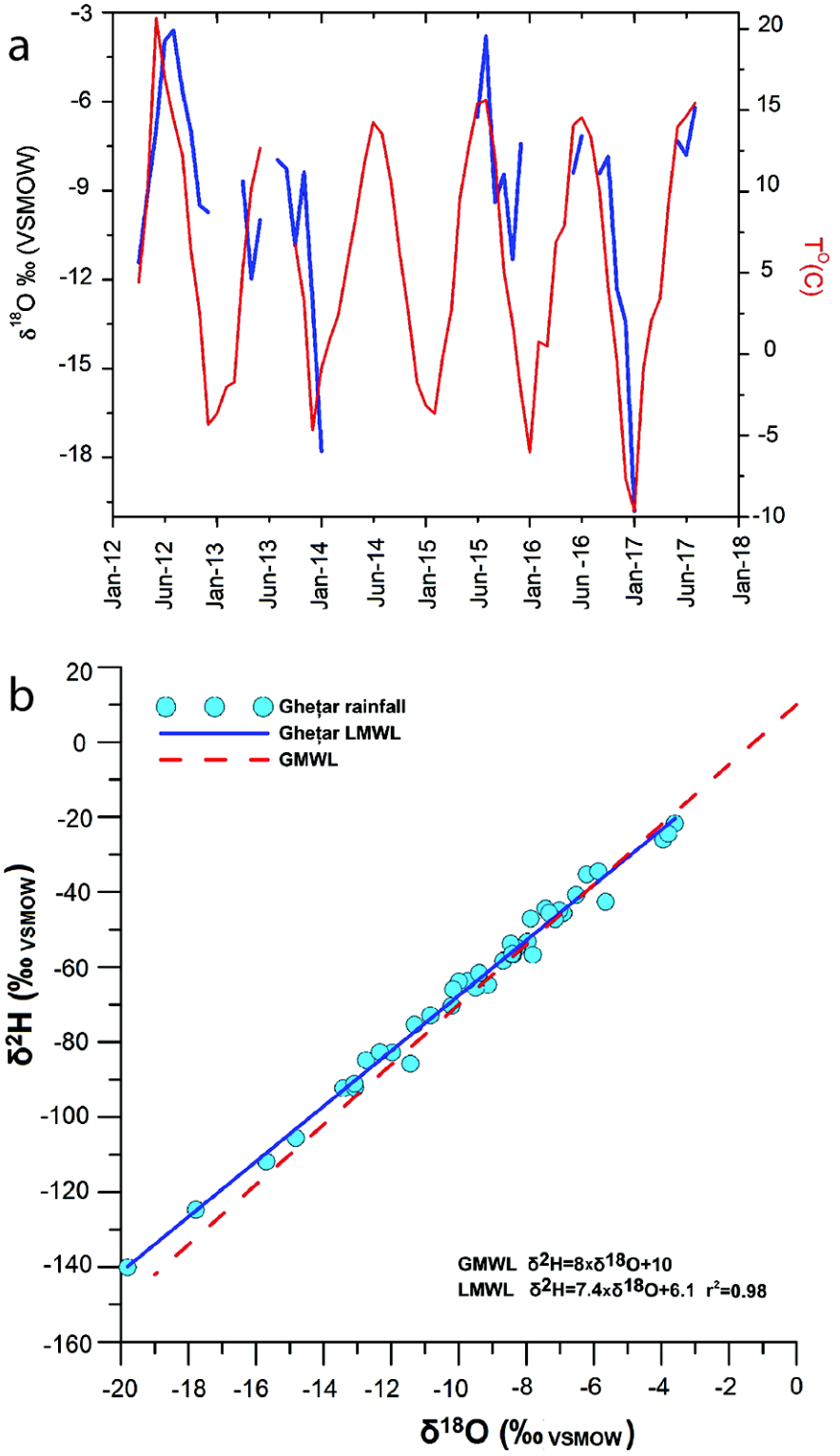

Figure 3. a) Temporal variability of $\delta^{18}O$ and $\delta^{2}H$ in precipitation and air temperature at Gheţar (10 km south of Focul Viu Ice Cave and at the same altitude), b) Local Meteoric Water Line of precipitation the same station, plotted against the Global Meteoric Water Line

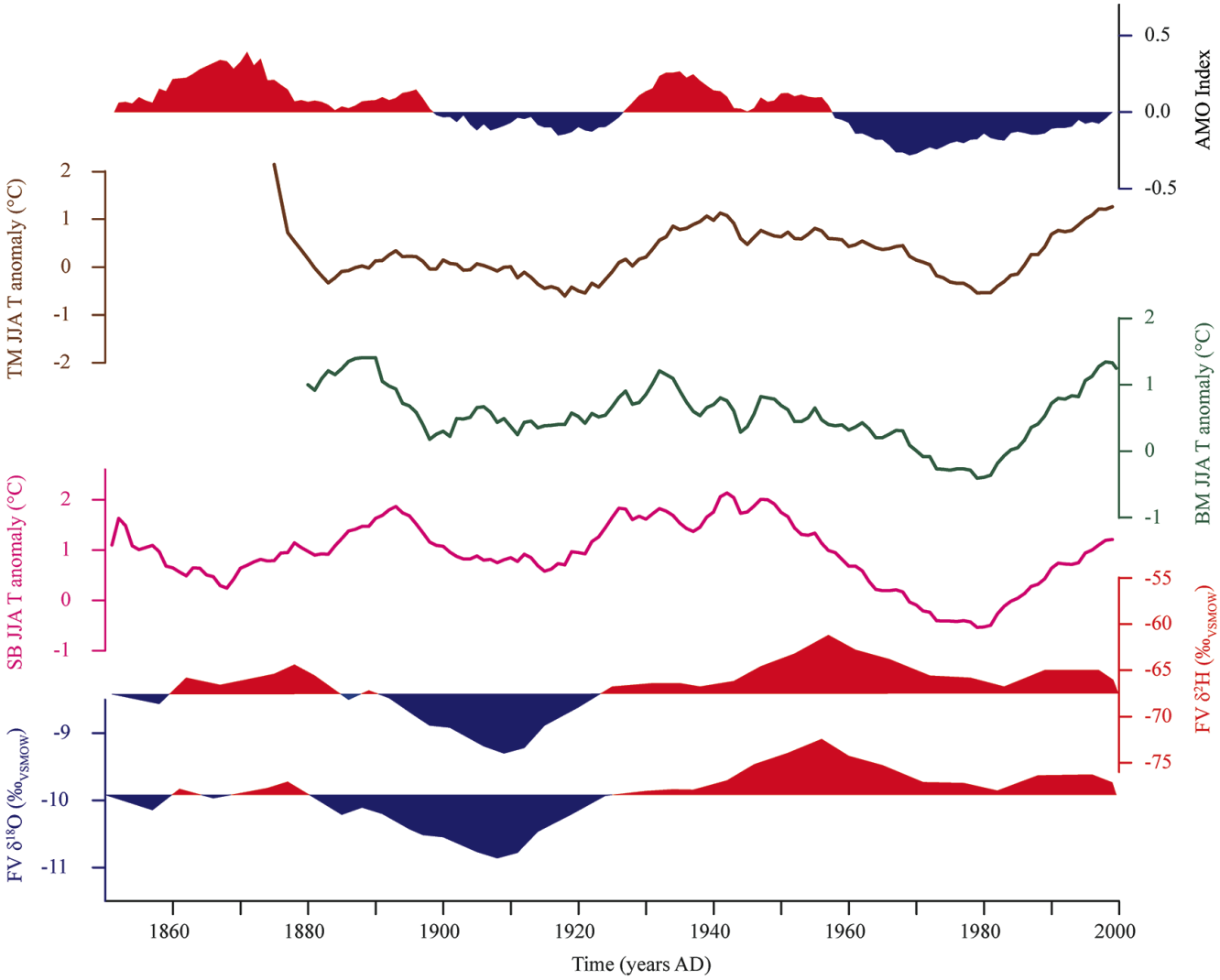

Figure 4. Temporal variability of the Atlantic Multidecadal Oscillation instrumental index, summer (JJA) air temperature (anomalies with respect to the 1961-1990 period) recorded at Baia Mare (BM), Timişoara (TM) and Sibiu (SB) weather stations and FV $\delta^{18}O$ and $\delta^{2}H$ (‰) during the instrumental period. The positive (red) and negative (blue) anomalies are shown against the 1850-2000 averages for the FV δ values.

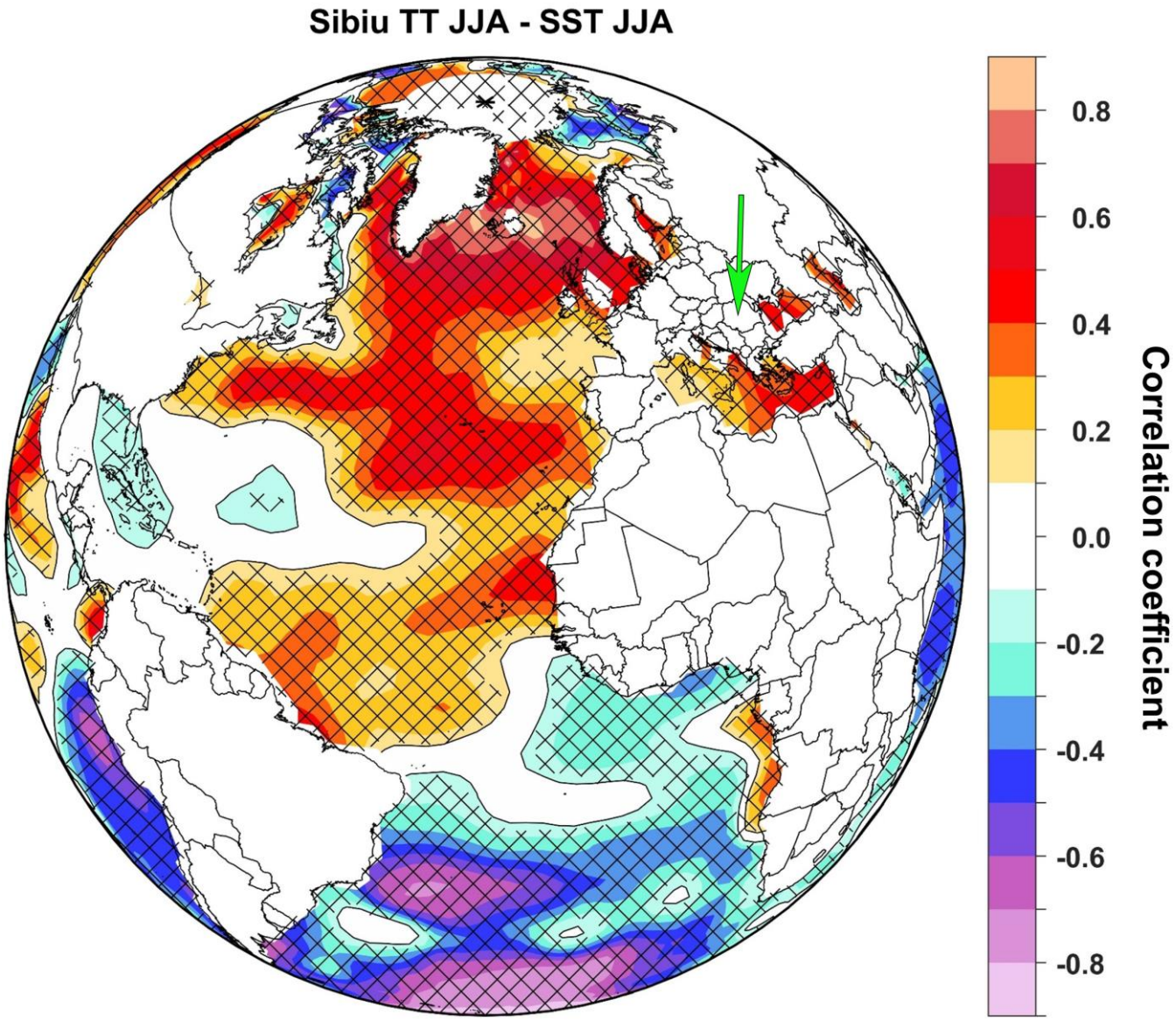

Figure 5. Spatial correlation map between Sea Surface Temperature (SST) and average summer (JJA June – July- August) air temperature at Sibiu (60 km south of Focul Viu Ice Cave, indicated by the green arrow) over the 1850-2011 period.

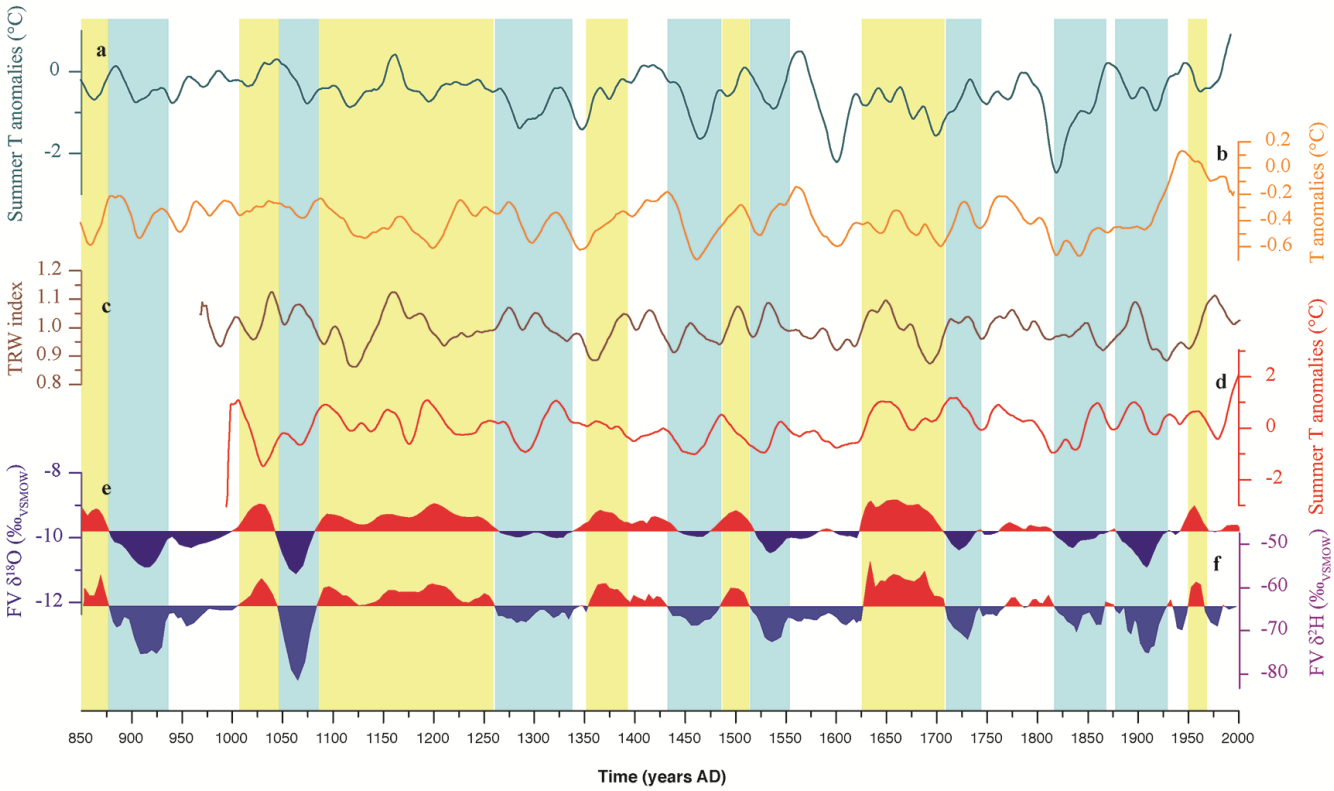

Figure 6. Summer climatic conditions recorded by $\delta^{18}O$ and $\delta^{2}H$ from FV ice core (panels e and f, bottom) and comparison with proxy indicator from the Northern Hemisphere: a) Central Europe summer temperature anomalies (against the 1901-2000 mean, Buntgen et al., 2011); b) Northern Hemisphere air temperature anomalies (against the 1961-1990 mean, D'Arrigo et al., 2006), c) Tree Ring Width Index from Albania, SE Europe (Seim et al., 2012), d) Summer temperature anomalies in Romania (against the 1961-1990 mean, Popa and Kern, 2009). Blue and yellow shading indicate cold and warm periods, respectively.

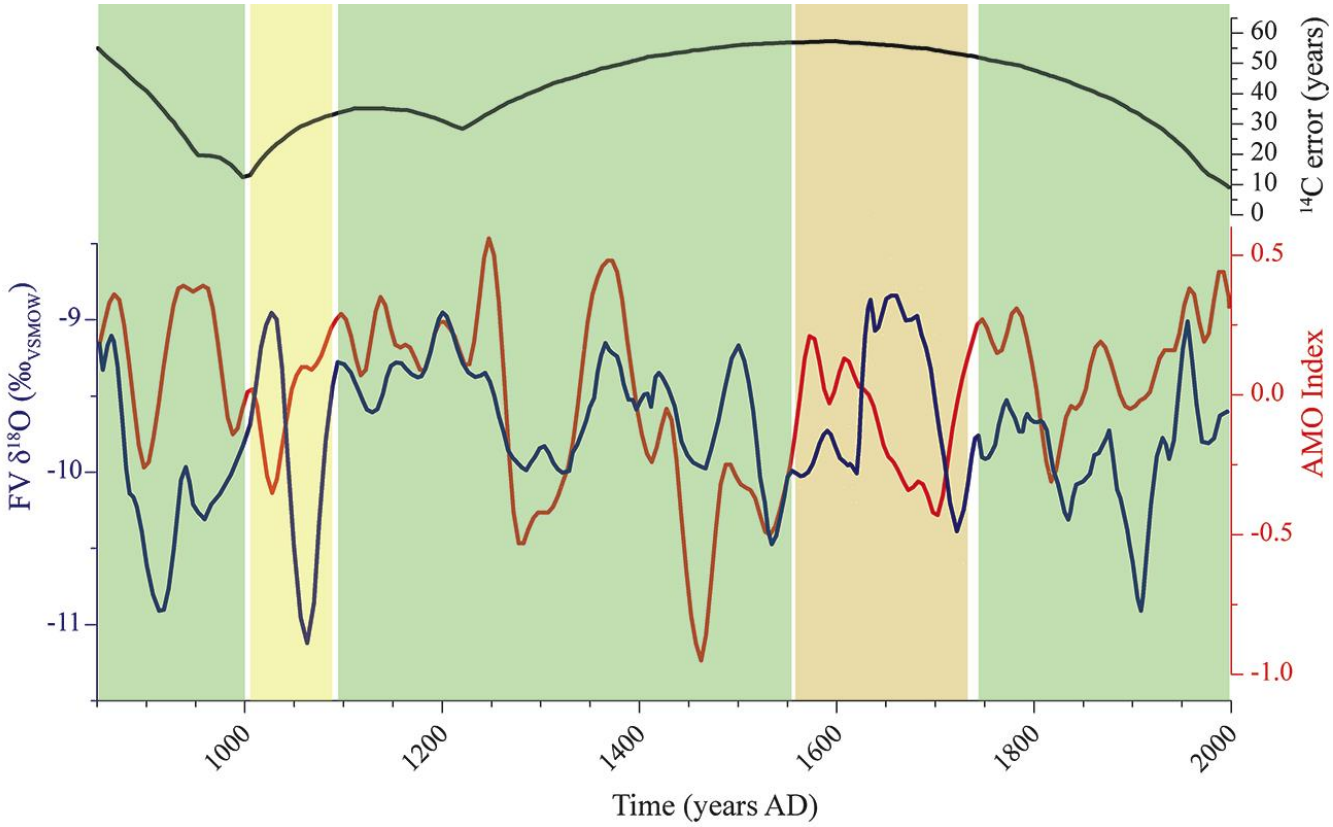

Figure 7. Temporal variability of the FV δ^{18}O (blue), the reconstructed AMO index (Wang et al., 2017) and the ^{14}C measurement uncertainty between AD 850 and 2000. Shading indicates the offset (in years) between the FV δ^{18}O and AMO index values: green – less than 20 years, yellow – between 20 and 50 years, orange – above 50 years.

Table 1. Radiocarbon data from the Focul Viu Ice Cave. Agreement indices for individual samples based on *P_Sequence* algorithm (Bronk Ramsey, 2008) are provided for accepted dates. Modeled ages for all dated depths are given as mean and sigma values, rounded to the nearest 5.

No	Lab code GdA-	Sample name	Depth (cm)	Material	Graphite mass (mg)	^{14}C age (BP)	Status and agreement index	Calibrated age ranges, unmodeled (AD)	Modeled age mean (AD) and 1 sigma
1	4889	FV'-5/19-22	21.5	needles and leaves, small fragments	0.86	-1410±25	Accepted (A=64%)	68.2% probability 1985AD (68.2%) 1988AD 95.4% probability 1958AD (9.6%) 1959AD 1985AD (85.8%) 1988AD	1975±20
2	5084	FV3/57-59	58	leaf fragments	0.54	525±30	Rejected	68.2% probability 1400AD (68.2%) 1435AD 95.4% probability 1320AD (14.9%) 1350AD 1390AD (80.5%) 1445AD	1890±45
3	4890	FV'/62-64	63	large wood fragment	1.00	875±25	Rejected	68.2% probability 1150AD (68.2%) 1215AD 95.4% probability 1045AD (18.1%) 1095AD 1120AD (4.6%) 1140AD 1145AD (72.7%) 1225AD	1880±45
4	5085	FV15/114-115	114.5	needle fragment, small	0.25	470±50	Rejected	68.2% probability 1405AD (68.2%) 1465AD 95.4% probability 1320AD (4.8%) 1350AD 1390AD (87.1%) 1520AD 1595AD (3.5%) 1620AD	1760±60
5	4891	FV3-10/155-156	155.5	small wood fragment	0.61	570±25	Rejected	68.2% probability 1320AD (40.2%) 1350AD 1390AD (28.0%) 1410AD 95.4% probability 1305AD (57.6%) 1365AD 1385AD (37.8%) 1420AD	1665±65
6	5086	FV6-4/232-235	232.5	needles and leaves, small fragments	0.14	1045±70	Rejected	68.2% probability 890AD (68.2%) 1040AD 95.4% probability 780AD (1.3%) 795AD	1490±65

								805AD (2.6%) 845AD 860AD (91.5%) 1160AD	
7	4892	FV7/276-278	277	large wood fragment	0.99	960±35	Rejected	68.2% probability 1020AD (22.4%) 1050AD 1080AD (34.5%) 1125AD 1135AD (11.3%) 1150AD 95.4% probability 1015AD (95.4%) 1160AD	1390±60
8	5087	FV8-3/308-310	311	small plant fragments	0.90	925±25	Rejected	68.2% probability 1040AD (42.8%) 1100AD 1120AD (25.4%) 1155AD 95.4% probability 1030AD (95.4%) 1165AD	1310±50
9	4893	FV9-14/348-350	349	leaves, fragments	0.99	780±35	Accepted (A=72%)	68.2% probability 1220AD (68.2%) 1270AD 95.4% probability 1190AD (95.4%) 1285AD	1225±30
10	5089	FV11-19/428-433	430.5	small plant fragments	0.61	1030±20	Accepted (A=97%)	68.2% probability 990AD (68.2%) 1020AD 95.4% probability 980AD (95.4%) 1030AD	1000±15
11	5090	FV12-2/444-446	445	small plant fragments	0.41	1140±20	Accepted (A=90%)	68.2% probability 885AD (19.7%) 905AD 915AD (48.5%) 965AD 95.4% probability 775AD (3.1%) 790AD 805AD (1.1%) 820AD 825AD (2.3%) 845AD 860AD (88.9%) 980AD	950±25